Italian Journal of Agrometeorology
Rivista Italiana di Agrometeorologia

Firenze University Press
www.fupress.com/ijam

OPEN ACCESS

Citation: A. Irvem, M. Ozbuldu (2022) Evaluation of the performance of CFSR reanalysis data set for estimating reference evapotranspiration (ET_0) in Turkey. *Italian Journal of Agrometeorology* (2): 49-61. doi: 10.36253/ijam-1325

Received: May 31, 2021

Accepted: December 1, 2022

Published: January 29, 2023

Data Availability Statement: All relevant data are within the paper and its Supporting Information files.

Competing Interests: The Author(s) declare(s) no conflict of interest.

Evaluation of the performance of CFSR reanalysis data set for estimating reference evapotranspiration (ET_0) in Turkey

Ahmet Irvem*, Mustafa Ozbuldu

Department of Biosystems Engineering, Faculty of Agriculture, Hatay Mustafa Kemal University, 31040, Antakya, Hatay, Turkey
*Corresponding author. E-mail: airvem@mku.edu.tr

Abstract. Evapotranspiration is a key process and a necessary parameter for hydrological, meteorological, and agricultural studies. However, the calculation of actual evapotranspiration is very challenging and costly. Therefore, reference evapotranspiration (ET_0) calculated using meteorological data is generally preferred over actual evapotranspiration. However, it is challenging to get complete and accurate data from meteorology stations in rural and mountainous regions. This study examined the suitability of the Climate Forecast System Reanalysis (CFSR) reanalysis data set as an alternative to meteorological observation stations to compute seasonal reference evapotranspiration for seven different climatic regions of Turkey. The ET_0 calculations using the CFSR reanalysis dataset for 1987-2017 were compared to data at 259 weather stations observed in Turkey. As a result of statistical evaluations, it has been determined that the most successful predicted season is winter (C' = 0.64-0.89, SPAEF= 0.63-0.81). The most successful estimations for this season were obtained from coastal areas with low elevations. The weakest estimations were obtained for the summer season (C' = 0.52-0.85, SPAEF= 0.59-0.77). These results show that the ET_0 estimation ability of the CFSR reanalysis dataset is satisfactory for the study area. In addition, it has been observed that CFSR tends to overestimate the observation data, especially in the southern and western regions. These findings indicate that the results of the ET_0 calculation using the CFSR reanalysis data set are relatively successful for the study area. However, the data should be evaluated with observation data before being used, especially in the summer models.

Keywords: CFSR reanalysis, Reference evapotranspiration, FAO56-PM, Turkey.

1. INTRODUCTION

Evapotranspiration (ET) is the total amount of water transferred to the atmosphere by evaporation from soil surfaces and transpiration from plant leaves (Tabari et al. 2013; Anderson et al. 2019). ET is the parameter that plays a crucial role in hydrological, meteorological, and agricultural studies, especially in planning water resources, programming irrigation time, and creating models. This parameter is measured in the field with different methods such as lysimeter (Gebler et al. 2015), Eddy-covariance method (Sun et al. 2008), Bowen ratio energy balance (Shi et al. 2008), scintillometer (Moorhead et al. 2017) and evaporation pans (Conceicao 2002). However, these procedures are quite costly and challenging to apply in wide basin conditions (Latrech et al. 2019).

Reference evapotranspiration (ET_0) is defined as the amount of water that can evaporate when the water in the soil is sufficient to meet the atmospheric moisture demand (Allen et al. 1998). The ET_0 is extremely useful for determining the atmospheric water demand of the area. Therefore, it is widely used in various applications such as irrigation planning, drought monitoring, and understanding the effects of climate change (Lang et al. 2017). Recently, numerous methodologies have been developed to determine ET_0 and actual evapotranspiration using meteorological data (Bandyopadhyay et al. 2012). These methods are mostly based on solar radiation (Priestley Taylor), temperature (Thornthwaite, Hargreaves, and Samani), and a combination of solar radiation and temperature (Penman-Monteith) (Seong et al. 2017; Purnadurga et al. 2019). Compared to other methods, the FAO56-PM method is considered a good way to estimate evapotranspiration globally (Sentelhas et al. 2010; Srivastava et al. 2013; Tabari et al. 2013; Tanguy et al. 2018).

Kite and Drooger (2000) assessed eight different ETo calculation methods and explained that the FAO56-PM method is most compatible with field observations. The FAO56-PM is a combination of physiological and aerodynamic methods that require climate factors like maximum and minimum temperature, wind speed, relative humidity, and solar radiation. However, there are no sufficient meteorological stations providing these data, particularly in developing countries, also these are not distributed uniformly (Alfaro et al. 2020). In addition, setting up and maintaining the meteorological station at these locations is quite costly (Tabari et al. 2013; Lang et al. 2017). Therefore, alternative data sources such as the reanalysis data set can be used to estimate ET_0 in case of a lack of required data. These datasets were generated using data from meteorology observation stations based on data assimilation methods, data from observation satellites, and weather estimate models (Purnadurga et al. 2019).

Reanalysis datasets with high precision and high spatiotemporal resolution have been widely used in recent years. (Alfaro et al. 2020). These are CFSR (Saha et al. 2010), NCEP/DOE (Kanamitsu et al. 2002), and NCEP/NCAR (Kalnay et al. 1996) datasets produced by NCEP, ERA-15 (Bromwich et al. 2005), ERA40 (Uppala et al. 2005) and ERA-Interim (Dee et al. 2011) datasets produced by ECMWF, JRA-55 (Ebita et al. 2011) datasets from the Japanese meteorology agency, and MERRA (Rienecker et al. 2011) datasets by NASA. The NCEP-CFSR uses numerical weather prediction techniques to identify atmospheric conditions with a resolution of 0.3125° x 0.3125° (~ 38 km). (Fuka et al. 2013). The most crucial advantage of CFSR is that it provides complete and continuous recording of climate data such as precipitation, temperature, solar radiation, relative humidity, and wind speed since 1979 (Auerbach et al. 2016).

Laurie et al. (2014) used reanalysis data as input in a hydrological model for the Mekong basin. They evaluated CFSR temperature data and model results. They indicated that CFSR temperature data gave satisfactory model results and it could be used for hydrological modeling studies if data is lacking. Tian et al. (2014) examined the usability of CFSv2 for seasonal estimation of evapotranspiration in different states of the USA. They explained that CFSv2-based ET estimations are more successful in cold seasons than warm seasons. Dile and Srinivasan (2014) assessed whether or not the CFSR dataset is appropriate for hydrologic modeling in their research in the Blue Nile River Basin. As a result of their study, the modeling with CFSR temperature and precipitation data gave similar results to the modeling using the data obtained from the observation stations and reported that the CFSR data set could be used in basins in the absence of observation stations. In another study, Alemayehu et al. (2015) evaluated the ability to calculate evapotranspiration with sufficient accuracy using different reanalysis datasets. They compared the ET_0 estimates calculated using the CFSR dataset with the results of the observation stations and reported that the CFSR dataset is a good alternative. Anderson et al. (2019) evaluated the usability of the CFSR reanalysis dataset in the context of a satellite-based remote sensing framework to map ET at high spatiotemporal resolution. They explained that the CFSR data has sufficient accuracy for use in ET modeling studies. Alfaro et al. (2020) calculated the evapotranspiration required for hydrological modeling with their study's CFSR reanalysis data set. They explained that the predictive performance of the CFSR dataset was good by evaluating the results obtained.

These studies show that reanalysis datasets such as CFSR are of sufficient quality and resolution to be used as inputs in basin modeling studies. In addition, this dataset can be an important alternative for overcoming problems encountered in obtaining meteorological observation data. This study aims to investigate the accuracy and usability of the CFSR reanalysis dataset to calculate ET_0 using the FAO56-Penman method in Turkey.

2. MATERIAL AND METHODS

2.1. Study area and meteorological data

Turkey is located between 36°-42° N and 26°-45° E. The total area is 779.452 square kilometers and the average altitude is 1141 meters. Turkey's climate is located between the temperate and sub-tropical zones. In the country, temperature and precipitation vary according to region due to factors such as the rugged terrain, the direction of the mountains, the fact that seas surround it on three sides, and the elevation increases from west to east. These factors cause different climate types to be seen. Depending on this situation, it has been traditionally accepted by Turkish climatologists since the beginning of the 20th century that there are seven climate regions in Turkey (Erinç, 1984). The locations of these regions are given in Figure 1.

Climate is generally harsh and cold in winter, especially in the Eastern Anatolia region, because of the high-pressure system from Siberia and the low-pressure system from Iceland. In summer, tropical air masses are generally more dominant by the effect of polar air masses moving towards northern latitudes. The Azores high-pressure system from the west of Europe and the Basra low-pressure system from the Persian Gulf are pretty effective in the summer season (Türkeş 2020).

The western and southern parts of the country have a Mediterranean climate, where precipitation peaks at the end of both winter and spring. Other parts generally have a continental climate with the highest precipitation in late spring or early summer. Annual precipitation varies from 295 to 2220 mm having an annual average of 648 mm (Deniz et al. 2011). The Black Sea and Mediterranean regions have more precipitation with the effect of air masses coming over the seas than the inner regions because the amount of precipitation decreases with the effect of the North and South Anatolian mountain ranges. The lowest temperatures are seen in the Eastern Anatolia Region due to the altitude, and the maximum temperatures are seen in the southern parts and the Mediterranean coasts (Katipoglu et al. 2021).

In this study, the calculated ET_0 using the FAO56-PM method, for each station was obtained from the "Vegetable Water Consumption Guide" published by the General Directorate of State Hydraulic Works and Agricultural Research and Policies (TAGEM). TAGEM used 30-year (1987-2017) daily minimum temperature, daily average temperature, daily maximum temperature, daily relative humidity, daily precipitation, daily wind speed,

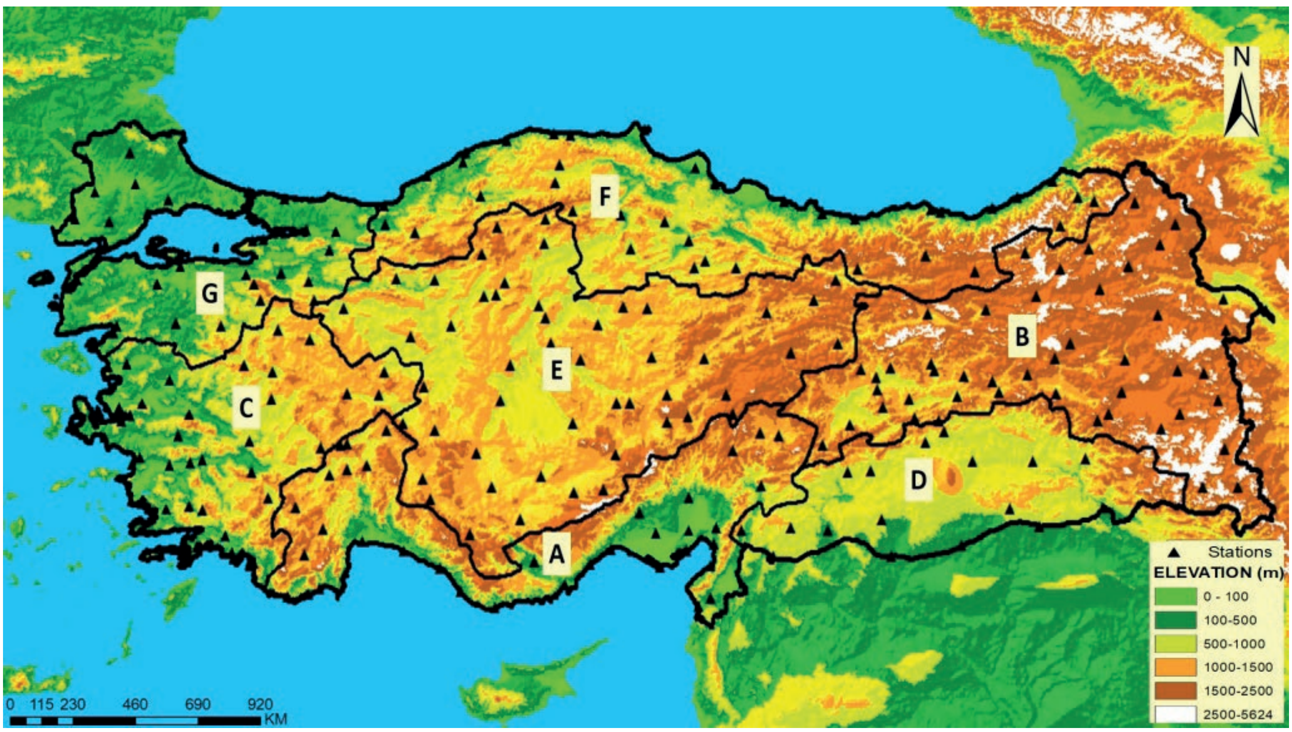

Figure 1. Location of meteorological stations and climate regions (The Mediterranean region (A), The Eastern Anatolia region (B), The Aegean region (C), The South-Eastern Anatolia region (D), The Central Anatolia region (E), The Black Sea region (F), The Marmara region (G)).

daily sunshine duration, and daily intensity of insolation data to calculate the ET_0. All data was obtained from 259 stations belonging to the General Directorate of Meteorology. The location of these stations is given in Figure 1. TAGEM declared that the daily data obtained from the observation stations were subjected to quality control and completed the missing data (TAGEM 2017).

2.2. CFSR reanalysis dataset

The CFSR reanalysis dataset contains the maximum and minimum temperatures (°C), precipitation (mm), wind speed (m s-1), relative humidity (%), and solar radiation (MJ m-2) from any location in the world (Dile and Srinivasan 2014; Irvem and Ozbuldu 2019). The spatial and temporal resolution of the CFSR is 0.35° (nearly 38 km) and 6 hours, respectively. CFSR datasets for Turkey (1987–2017) were obtained via the internet (https://rda.ucar.edu/).

2.3. FAO56-PM method

Penman (1948) developed an evaporation formula for open water surfaces based on climatic data. Monteith (1976) adjusted this formula by adding aerodynamics and surface strength factors and called the Penman-Monteith equation (PM). PM calculated using the given equation.

$$ET_0 = \frac{0.408\,\Delta\,(R_n - G) + \frac{900\,\gamma}{T+273}\,u_2\,(e_s - e_a)}{\Delta + \gamma\,(1 + 0.34\,u_2)} \tag{1}$$

where; ET_0 is daily referenced ET (mm day^{-1}), Δ is the slope of the relationship between saturation vapor pressure and mean daily air temperature (kPa °C^{-1}), R_n is the net radiation at the crop surface (MJ m^{-2} day^{-1}), G is the soil heat flux density (MJ m^{-2} day^{-1}), γ is the psychrometric constant which depends on the altitude of each location (kPa °C^{-1}), T is the mean daily air temperature (°C), u_2 is the wind speed at 2 m height (m s^{-1}); e_s is the saturation vapor pressure (kPa); e_a is the actual vapor pressure (kPa).

2.4. Evaluation criteria

The five statistical measures were used to evaluate the accuracy of the ET_0 estimation by comparing the calculated ET_0 using CFSR dataset against the calculated ET_0 using meteorological station data. These are the coefficient of determination (R^2), root-mean-square error (RMSE), PBias (percent bias), and the performance index (C') and SPAtial Efficiency (SPAEF).

R^2 shows to what extent the ET_0 estimates calculated with the CFSR dataset are similar to the ET_0 values calculated with the observation data. R^2 varies between 0 and 1, higher values indicate less error variation. Generally, values above 0.50 are considered acceptable (Santhi et al. 2001; Moriasi et al. 2007) and calculated based on Eq 2.

$$R^2 = \left(\frac{n\sum(O_i M_i) - (\sum O_i)(\sum M_i)}{\sqrt{(n(\sum O_i^2) - (\sum O_i)^2)(n(M_i^2) - (\sum M_i)^2)}} \right)^2 \tag{2}$$

The value of RMSE should always be positive and it is desired to be close to zero. This indicates that the lower the value, the better the model will perform. RMSE provides performance information for correlations by comparing the difference between model results and observed values (Piñeiro et al. 2008). RMSE is calculated by Eq. 3.

$$RMSE = \sqrt{\frac{1}{n}\sum(Predict_i - Obs_i)^2} \tag{3}$$

PBias is used to determine how far the model predicted values are in the negative or positive direction from the observed values. Whereas positive values indicate that the observed values are higher than the simulated values, negative values indicate the opposite situation (Gupta et al. 1999). PBias is determined by Eq. 4.

$$PBias = 100\,(\sum Obs_i - Predict_i \,/\, \sum Obs_i\,) \tag{4}$$

The performance index (C') was calculated by combining accuracy and precision criteria into the relationship between the model and the predictive data. The Pearson linear correlation coefficient, which measures the degree and direction of distribution among variables, was used as a precision criterion. The Willmott's index of agreement was chosen as an accuracy criterion because it measures the degree of fit between the predicted and observed data. The performance index of the model was computed by Eq. 5 and evaluated using Table 1 (Santos et al. 2020).

C' = *Correlation Coefficient (CC)* * Willmott's index of agreement(*d*) (5)

The Willmott index of agreement (d) shows the degree of fit between observed and predicted measurements between 0 and 1. The closer the result is to 1, the better the model performance is determined (Willmott 1981; Tran et al. 2020). It is calculated by Eq. 6.

Table 1. Model performance evaluation table (Moriasi et al. 2007; Santos et al. 2020).

Classification	C'	PBias
Very Good	0.75 - 1.00	< 10
Good	0.65 - 0.75	10 - 15
Satisfactory	0.55 - 0.65	15 - 25
Unsatisfactory	< 0.55	> 25

$$d = \frac{\sum(Obs_i - Predict_i)^2}{\sum([Predict_i - Obs_{mean}] + [Obs_i - Obs_{mean}])^2} \tag{6}$$

SPAEF was developed by Demirel et al. (2018) as a holistic and balanced assessment method that uses various aspects for a comprehensive assessment. SPAEF value is between −∞ and 1. The closer the result is to 1, the higher the prediction success. The SPAEF values are computed by Eq. 7.

$$SPAEF = 1 - \sqrt{(\alpha - 1)^2 + (\beta - 1)^2 + (\gamma - 1)^2}$$

$$\alpha = \rho(obs, sim), \beta = \left(\frac{\sigma_{sim}}{\mu_{sim}}\right) \Big/ \left(\frac{\sigma_{obs}}{\mu_{obs}}\right), \gamma = \frac{\sum_{j=1}^{n} \min(K_j, L_j}{\sum_{j=1}^{n} K_j} \tag{7}$$

where, α represents the Pearson correlation coefficient, β is the fraction of the coefficient of variation representing spatial variability, γ is the histogram intersection for the given histogram K of the observed pattern and the histogram L of the simulated pattern, each containing n bins (Swain and Ballard, 1991). Correlation is a statistical measure that allows two variables to be compared. The CV ratio indicates whether the spatial variability is adequately represented. Histo match value is an indicator of spatial variability that is not present in high and low areas despite satisfactory correlation and spatial variability (Koch et al. 2018).

3. RESULTS AND DISCUSSION

The mean seasonal and mean annual ET_0 were estimated for each observation station using CFSR reanalysis data set which consists of the daily meteorological data from 1987 to 2017. These estimates were compared with the ET_0 values calculated by TAGEM using data from meteorological ground observation stations. The accuracy and usability of the CFSR reanalysis dataset were evaluated using different statistical evaluation criteria. In addition, maps were created using the IDW interpolation technique to show the areal distributions of long-term annual averages of ET_0 results for different seasons.

3.1. Results of ET_0 estimates for the winter season

The ETo estimation results obtained using the CFSR data set for the winter season (December, January, and February) were compared with the observed data separately for each climate region. The performance evaluation results are given in Table 2.

Results show that the estimation performance is higher in regions close to the sea and lower in regions with high elevation. The Performance Index (C') was calculated as 0.89 in the Mediterranean region at the highest, and 0.64 in the Eastern Anatolia region at the lowest. In general, the performance of ET_0 estimations using CFSR data for the winter season was determined to be high (C' > 0.65).

Similar to the Performance Index results, the highest SPAEF values were calculated at 0.81, 0.75, and 0.73 for the Mediterranean, the Black Sea, and the Aegean regions, respectively. Thus, the best estimations of ET_0 for the winter season have been seen in the coastal regions in terms of spatial variability and distribution.

Spatial distribution of estimated and observed ET_0 values for the winter season were classified into 6 categories between 20 and 250 mm as shown in the map (Fig. 2).

Table 2. Performance evaluation results for the winter season.

Regions	R^2	RMSE (mm season^{-1})	PBias (%)	d	C'	SPAEF
The Mediterranean region	0.87	14.87	-5.46	0.96	0.89	0.81
The Eastern Anatolia region	0.72	16.09	23.03	0.76	0.64	0.63
The Aegean region	0.82	20.01	-13.92	0.88	0.80	0.73
The South-Eastern Anatolia region	0.72	8.25	-2.35	0.91	0.78	0.63
The Central Anatolia region	0.76	10.18	3.39	0.90	0.79	0.64
The Black Sea region	0.84	9.27	-0.15	0.96	0.88	0.75
The Marmara region	0.77	5.50	-7.68	0.92	0.81	0.65

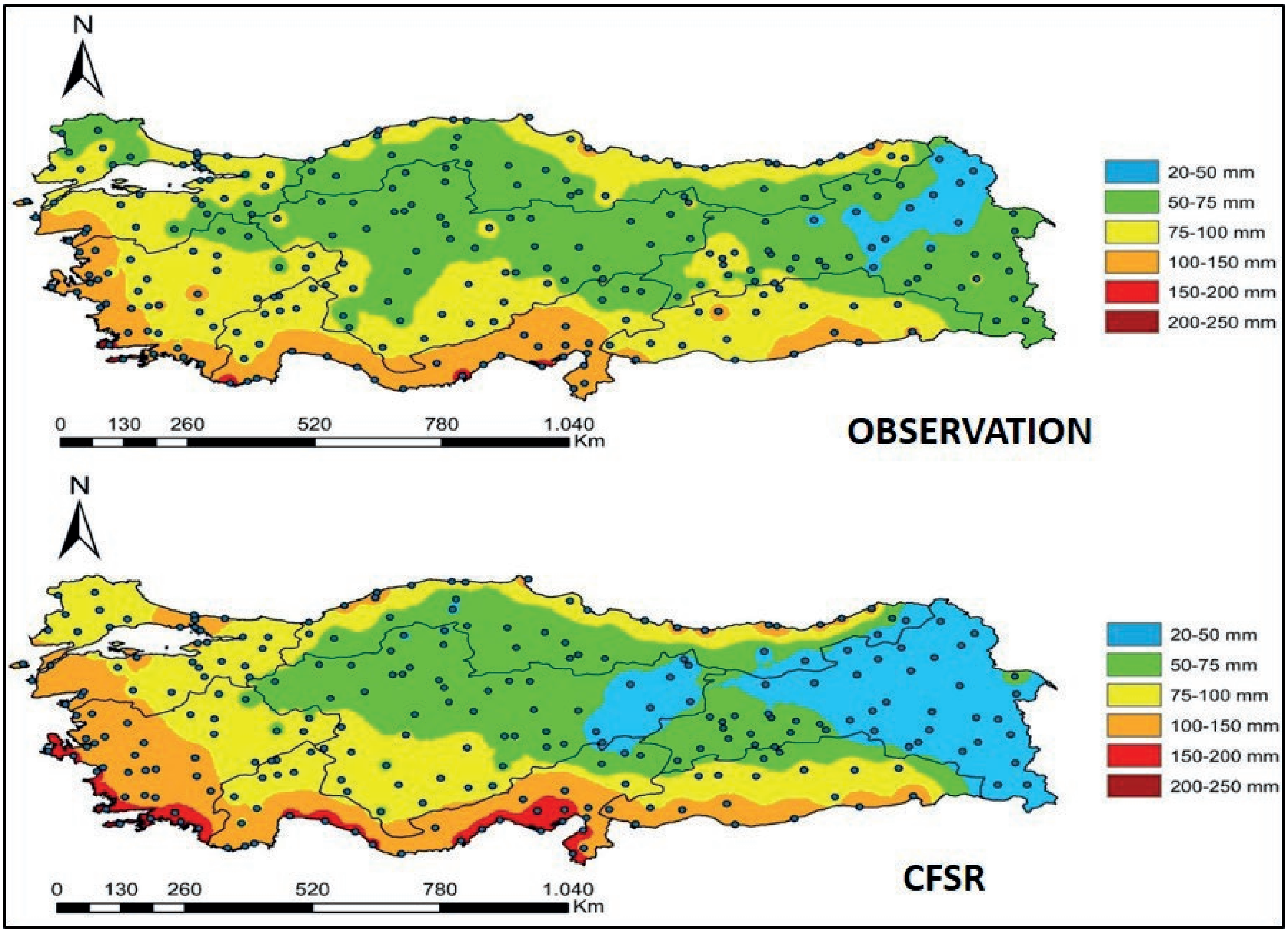

Figure 2. Average long-term ET_0 map for the winter season a) observation b) CFSR.

The CFSR reanalysis dataset has relatively high temperature and solar radiation data in the south and west regions, unlike the eastern region. Consequently, the results of CFSR estimations are better in regions having higher temperatures and solar radiation. PBias values for most stations are negative. ET_0 estimation using CFSR in five regions was overestimated for the winter season. On the other hand, it was underestimated in the Eastern Anatolia (23.03) and Central Anatolia (3.39) regions. Bhattacharya et al. (2020) evaluated reanalysis and global meteorological products in the Beas River Basin of Northwestern Himalaya. They compared CFSR and observed temperature data and explained that the temperature differences between CFSR and observed temperature data are less in the western region where the temperature is higher than in the eastern region.

The R^2 value calculated between 0.72-0.87 as seen in Table 2. This shows that the CFSR reanalysis dataset has a good correlation with the observation data. R^2 values between 0.50-0.99 are considered good estimates for hydrological studies (Alfaro et al. 2020).

3.2. Results of ET_0 estimates for the spring season

The ET_0 estimation results obtained using the CFSR data set for the spring season (March, April, and May) were compared with the observed data separately for each climate region. The performance evaluation results for the spring are given in Table 3.

Performance Index (C') was calculated as 0.81 in the Black Sea region at the highest, and 0.72 in the The South-Eastern Anatolia region at the lowest. In general, the performance of ET_0 estimations using CFSR data for the spring season was determined to be high (C' > 0.70).

Similar to the Performance Index results, the highest SPAEF values were calculated at 0.84, 0.79, and 0.72 for the Black Sea, the Marmara and the Central

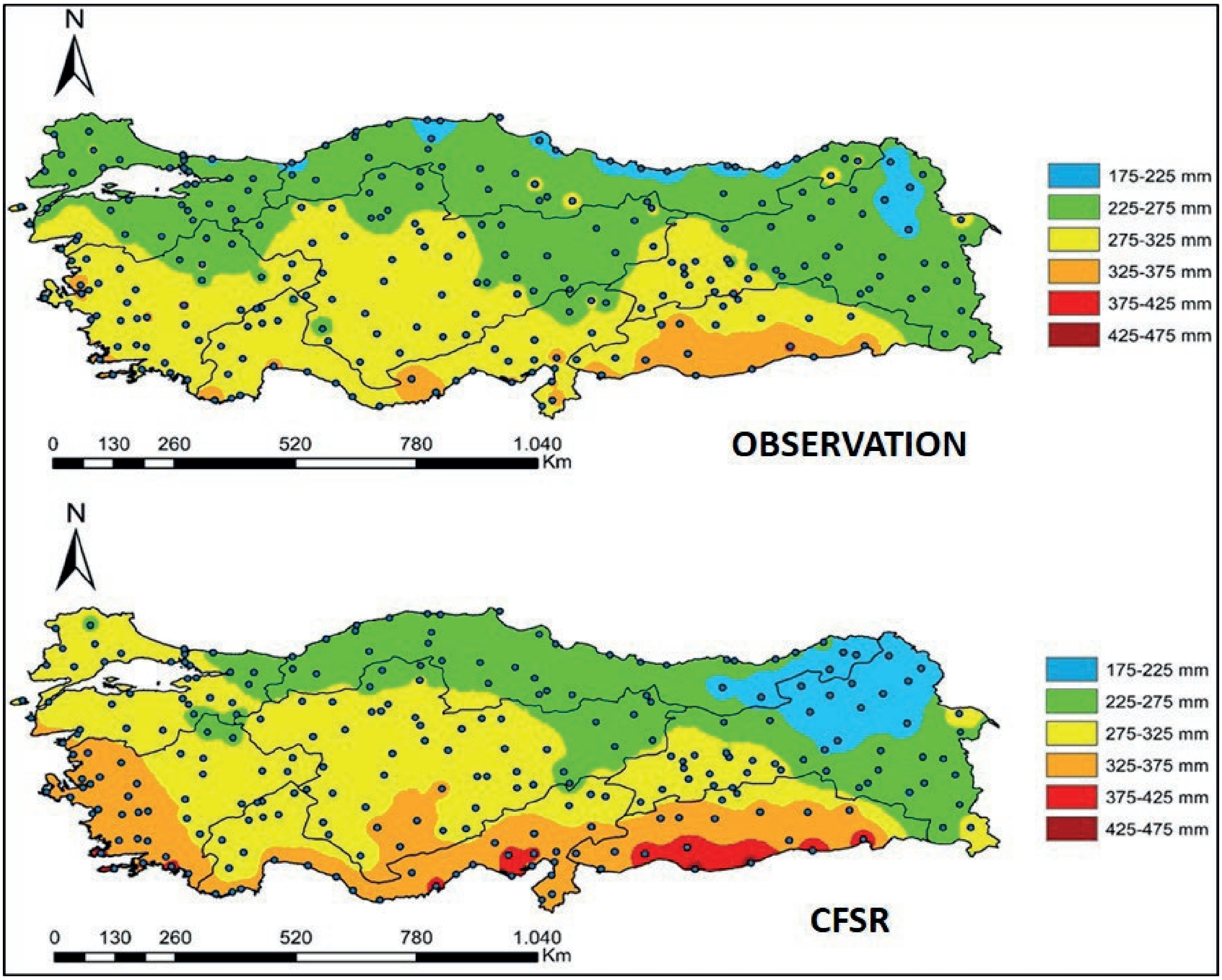

Figure 3. Average long-term ET_0 map for the spring season a) observation b) CFSR.

Table 3. Performance evaluation results for the spring season.

Regions	R2	RMSE (mm season-1)	PBias (%)	C'	SPAEF
The Mediterranean region	0.75	15.40	-3.69	0.77	0.67
The Eastern Anatolia region	0.72	22.23	-5.15	0.73	0.63
The Aegean region	0.75	20.34	-4.61	0.79	0.63
The South-Eastern Anatolia region	0.70	15.27	-5.47	0.72	0.55
The Central Anatolia region	0.77	14.75	-0.78	0.79	0.72
The Black Sea region	0.82	19.30	-2.01	0.81	0.84
The Marmara region	0.79	21.28	-2.64	0.75	0.79

Anatolia regions, respectively. Thus, the best estimations of ET_0 for the spring season have been seen in the northern regions in terms of spatial variability and distribution.

Spatial distribution of estimated and observed ET_0 values for the spring season were classified into 6 categories between 175 and 475 mm as shown in the map (Figure 3). Same as winter season, the results of CFSR

Table 4. Performance evaluation results for the summer season.

Regions	R^2	RMSE (mm season^{-1})	PBias	C'	SPAEF
The Mediterranean region	0.69	72.27	-12.10	0.53	0.61
The Eastern Anatolia region	0.63	76.47	-11.07	0.61	0.59
The Aegean region	0.74	41.06	-7.34	0.71	0.70
The South-Eastern Anatolia region	0.67	69.98	-13.04	0.52	0.61
The Central Anatolia region	0.75	38.96	-6.17	0.74	0.74
The Black Sea region	0.82	22.38	-2.50	0.85	0.77
The Marmara region	0.71	32.90	-2.17	0.75	0.66

estimations for spring are better in regions having higher temperatures and solar radiation. PBias values for most stations are negative. ET_0 estimation using CFSR in all regions was overestimated for the spring season. The R^2 values calculated between 0.70-0.82 as seen in Table 3. This shows that the CFSR reanalysis dataset has a good correlation with the observation data for spring season.

3.3. Results of ET_0 estimates for the summer season

The ET_0 estimation results obtained using the CFSR data set for the winter season (June, July, and August) were compared with the observed data separately for each climate region. The performance evaluation results are given in Table 4.

The Performance Index (C') was calculated as 0.85 in the Black sea region at the highest, and 0.52 in the The South-Eastern Anatolia region at the lowest. In general, the performance of ET_0 estimations using CFSR data for the summer season was determined to be acceptable (C' > 0.55) in five regions but two region have poor estimation performance. These two regions Mediterranean and The South-Eastern Anatolia regions have relatively higher temperature.

Similar to the Performance Index results, the highest SPAEF values were calculated at 0.77, 0.74, and 0.70 for the Black Sea, The Central Anatolia and the Aegean regions, respectively. Thus, the best estimations of ET_0 for the summer season have been seen in the Northern regions in terms of spatial variability and distribution. Spatial distribution of estimated and observed ET_0 values for the winter season were classified into 6 categories between 300 and 900 mm as shown in the map (Figure 4).

When the predictions made by the CFSR for the summer season are compared with the observation data, the differences between the results are higher than in other seasons as seen in Figure 4. The reason for this thought is that temperature and solar radiation increase considerably in the summer months and the CFSR reanalysis data set cannot accurately predict these changes. Tian et al. (2014) reported that the estimates obtained for the winter season were more successful than the summer seasons. They explained that this is due to the fact that more convective heating occurs in summer than in winter. Because this type of convection can produce different weather conditions on a small scale, it may not be detected by reanalysis due to coarse solubility. PBias value was calculated from -2.17 to 12.10 for the summer season. It shows that the CFSR reanalysis made higher estimates in summer than winter and spring, but estimated ET_o for the summer is still in acceptable (<± 25) ranges.

The R^2 values calculated between 0.63-0.82 as seen in Table 4. This shows that the CFSR reanalysis dataset has a good correlation with the observation data for summer season. Although ET_o estimates are acceptable in terms of R^2 (>0.50), the ET_o estimation of the CFSR reanalysis dataset underperforms in the summer due to the decrease in solar radiation and temperature prediction capabilities (Bhattacharya et al. 2020). The reason can be explained that more convective warming occurs in summer compared to other seasons. This type of convection may cause the formation of different weather conditions on a small scale that CFSR cannot predict due to its coarse resolution (Tian et al., 2014). Using the CFSR data set directly on models for the summer months will result in unsuccessful simulation results. For this reason, preliminary procedures that will reduce this dataset to a regional scale should be applied and reevaluated before using it.

3.4. Results of ET_0 estimates for the autumn

The ET_0 estimation results obtained using the CFSR data set for the autumn season (September, October, and November) were compared with the observed data separately for each climate region. The performance evaluation results are given in Table 5.

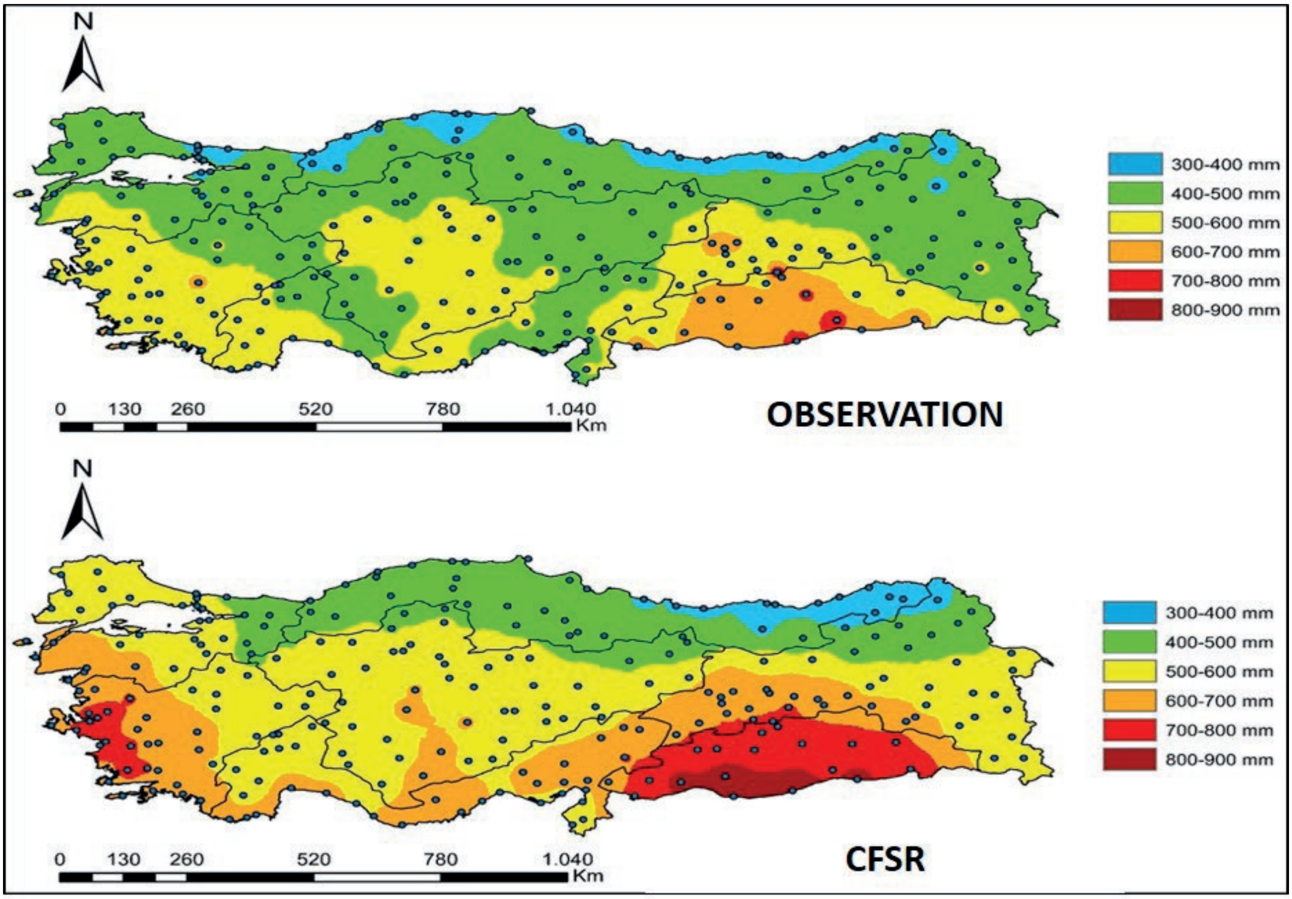

Figure 4. Average long-term ET_0 map for the summer season a) observation b) CFSR.

Performance Index results (C') was calculated as 0.86 in the Black Sea region at the highest, and 0.69 in The South-Eastern Anatolia region at the lowest. In general, the performance of ET_0 estimations using CFSR data for the autumn season was determined to be high (C' > 0.65). Similar to the Performance Index results, the highest SPAEF values were calculated at 0.80, 0.77, and 0.73 for the Mediterranean, the Black Sea, and the Marmara regions, respectively. Thus, the best estimations of ET_0 for the autumn season have been seen in the coastal regions in terms of spatial variability and distribution.

Spatial distribution of estimated and observed ET_0 values for the winter season were classified into 6 categories between 300 and 900 mm as shown in the map (Figure 5). PBias value was calculated from -0.31 to -8.83 for the autumn season. The R^2 values calculated between

Table 5. Performance evaluation results for the autumn season.

Regions	R^2	RMSE (mm season^{-1})	Pbias (%)	C'	SPAEF
The Mediterranean region	0.85	11.16	-4.54	0.84	0.80
The Eastern Anatolia region	0.68	22.52	-8.83	0.72	0.58
The Aegean region	0.80	15.73	-5.83	0.77	0.70
The South-Eastern Anatolia region	0.75	28.73	-4.60	0.69	0.60
The Central Anatolia region	0.84	21.09	-6.50	0.84	0.72
The Black Sea region	0.89	15.45	-0.31	0.86	0.77
The Marmara region	0.77	12.09	-2.82	0.82	0.73

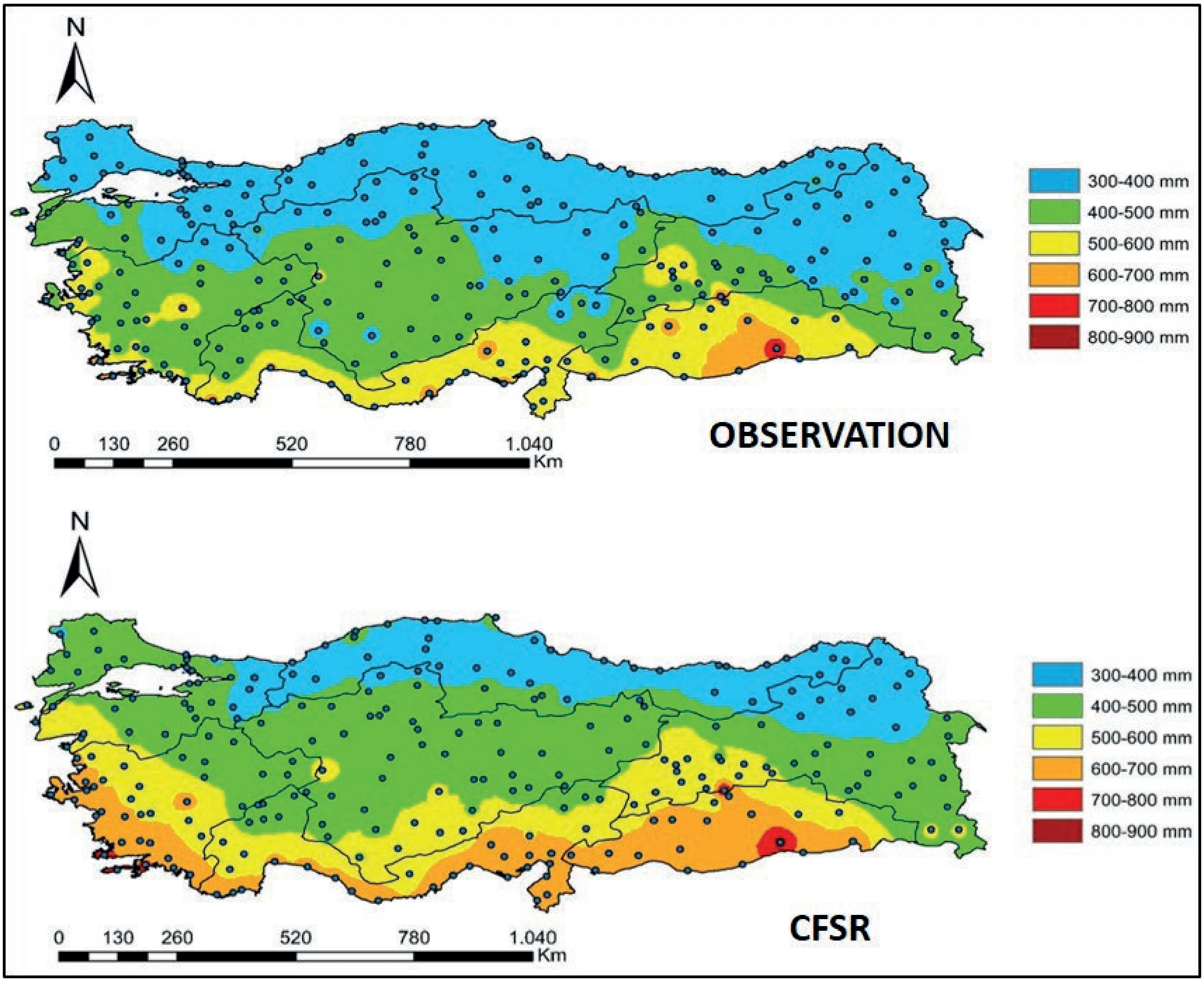

Figure 5. Average long-term ET_0 map for the autumn season a) observation b) CFSR.

0.68-0.89 as seen in Table 5. This shows that the CFSR reanalysis dataset has a good correlation with the observation data for autumn season.

When evaluated in general, it was determined that the ETo estimations for the winter and autumn seasons were more successful than the spring and summer seasons. Tian et al. (2014) explained that the ETo estimations are performed more accurately in the winter season using the CFSR data set for regions with missing ET_o.

While the ET_0 estimations calculated for the coastal regions during the cold seasons performed better, the estimation performance was found to be low in the inner regions with high altitudes. In the spring and summer seasons, the estimate performance was generally lower due to the higher temperature and solar radiation. Especially in summer, estimate performance was underestimated in the southern regions. The CFSR reanalysis dataset tends to overestimate ET_o than the observation data due to increased temperature and solar radiation (Srivastava et al., 2013; Paredes et al., 2017; Tian et al., 2018).

The best estimation performance results are obtained for the coastal regions because the temperature differences in these regions are less than in inner regions due to the effect of the sea in winter. On the other hand, it was understood that the worst estimation results were obtained, especially in the Eastern Anatolia region, due to the difference in temperature values depending on the altitude Bhattacharya et al. (2020) were found similar results in their study carried out in the Beas River Basin of Northwestern Himalaya. It was determined that CFSR was more successful in estimating ETo for northern regions in the spring season. It has been understood that the temperature difference in these regions is less in March, April, and May than in the southern regions, which affects the accuracy of the estimations

4. CONCLUSION

ETo is a very important parameter for hydrological, meteorological, and agricultural studies. However, it is very difficult to obtain the meteorological data for the calculation or estimation of this parameter in developing countries for the required regions. In this study, ETo was estimated by the FAO56-PM method using observed and CFSR data set for Turkey. The accuracy of the seasonal estimations was evaluated statistically by comparing it with the ETo calculated with the meteorological ground observation station data by TAGEM.

As a result of regional evaluations, it has been determined that the most successful predicted season is winter. The most successful estimations for this season were obtained from coastal areas with low elevation. The weakest estimations were obtained for the summer season. Especially with the higher temperature and the solar radiation, very poor estimates were obtained in the southern regions. The ETo estimation ability of the CFSR reanalysis dataset is generally satisfactory for the study area. PBias value was calculated as negative for almost all seasons.

It has been observed that CFSR tends to overestimate the observation data, especially in the southern and western regions. According to all results, the CFSR reanalysis data set is a good potential data source. However, it is recommended to evaluate the data with observation data before being used especially in summer seasons and to be used after regionalization with downscaling methods before being used in models.

REFERENCES

Alemayehu T, van Griensven A, Bauwens W (2016) Evaluating CFSR and WATCH data as input to SWAT for the estimation of the potential evapotranspiration in a data-scarce Eastern-African catchment. J Hydrol Eng 21(3):1–16. https://doi.org/10.1061/(ASCE)HE.1943-5584.0001305

Alfaro MDM, Lopes I, Montenegro AAA, Leal BG (2020) CFSR- NCEP performance for weather data forecasting in the Pernambuco Semiarid, Brazil. DYNA 87(215):204-213. http://doi.org/10.15446/dyna.v87n215.89952

Allen RG, Pereira SL, Raes D, Smith M (1998) Crop evapotranspiration. Guidelines for computing crop water requirements. FAO Irrigation and Drainage Paper 56, Rome, pp 300

Anderson M, Diak G, Gao F, Knipper K, Hain C, Eichelmann E, Hemes K, Baldocchi D, Kustas W, Yang YJRS (2019) Impact of insolation data source on remote sensing retrievals of evapotranspiration over the California Delta. Remote Sens 11:216. https://doi.org/10.3390/rs11030216

Auerbach DA, Easton ZM, Walter MT, Flecker AS, Fuka DR (2016) Evaluating weather observations and the Climate Forecast System Reanalysis as inputs for hydrologic modelling in the tropics. Hydrol Process 30(19):3466–3477. https://doi.org/10.1002/hyp.10860

Bandyopadhyay A, Bhadra A, Swarnakar RK, Raghuwanshi NS, Singh R (2012) Estimation of reference evapotranspiration using a user-friendly decision support system: DSS_ET. Agr Forest Meteorol 154:19–29. https://doi.org/10.1016/j.agrformet.2011.10.013

Bromwich DH, Wang SH (2005) Evaluation of the NCEP-NCAR and ECMWF 15- and 40-yr reanalyses using rawinsonde data from two independent Arctic field experiments. Mon Weather Rev 133:3562–3578. https://doi.org/10.1175/MWR3043.1

Conceição MAF (2002) Reference evapotranspiration based on Class A-pan evaporation. Sci Agric. 59(3):417-420. https://doi.org/10.1590/S0103-90162002000300001

Dee DP, Uppala S, Simmons A, Berrisford P, Poli P, Kobayashi S, Andrae U, Balmaseda M, Balsamo G, Bauer P (2011) The ERA-Interim reanalysis: Configuration and performance of the data assimilation system. Q J Roy Meteor Soc 137:553–597. https://doi.org/10.1002/qj.828

Demirel MC, Mai J, Mendiguren G, Koch J, Samaniego L, Stisen S (2018) Combining satellite data and appropriate objective functions for improved spatial pattern performance of a distributed hydrologic model. Hydrol Earth Syst Sci 22(2): 1299–1315. https://doi.org/10.5194/hess-22-1299-2018

Deniz A, Toros H, Incecik S (2011) Spatial variations of climate indices in Turkey. Int J Clim. 31(3): 394–403. https://doi.org/10.1002/joc.2081

Dile YT, Srinivasan R (2014) Evaluation of CFSR Climate Data for Hydrologic Prediction in Data-Scarce Watersheds: An Application in the Blue Nile River Basin. J Am Water Resour As 50:1226–1241. https://doi.org/10.1111/jawr.12182

Ebita A, Kobayashi S, Ota Y, Moriya M, Kumabe R, Onogi K, Harada Y, Yasui S, Miyaoka K, Takahashi K, Kamahori H, Kobayashi C, Endo H, Soma M, Oikawa Y, Ishimizu T (2011) The Japanese 55-year Reanalysis "JRA-55": An interim report. SOLA 7:149–152. https://doi.org/10.2151/sola.2011-038

Erinc S. (1984). Climatology and its methods, 3rd edition. Istanbul, Gur-ay Pres Inc. (in Turkish)

Fuka DR, Walter MT, MacAlister C, Degaetano AT, Steenhuis TS, Easton ZM (2013) Using the Climate Forecast System Reanalysis as weather input data for watershed models. Hydrol Process 28:5613–5623. https://doi.org/10.1002/hyp.10073

Gebler S, Hendricks Franssen HJ, Putz T, Post H, Schmidt M, Vereecken H (2015) Actual evapotranspiration and precipitation measured by lysimeters: A comparison with eddy covariance and tipping bucket. Hydrol Earth Syst Sc 19:2145–2161. https://doi.org/10.5194/hess-19-2145-2015

Gupta HV, Sorooshian S, Yapo PO (1999) Status of automatic calibration for hydrologic models: comparison with multilevel expert calibration. J Hydrol Eng 4(2):135–143. https://doi.org/10.1061/(ASCE)1084-0699(1999)4:2(135)

Irvem A, Ozbuldu M 2019 Evaluation of Satellite and Reanalysis Precipitation Products Using GIS for All Basins in Turkey. Adv Meteorol 2019(4820136):1–11. https://doi.org/10.1155/2019/4820136

Kalnay E, Kanamitsu M, Kistler R, Collins W, Deaven D, Gandin L, Iredell M, Saha S, White G, Woollen J, Zhu Y, Chelliah M, Ebisuzaki W, Higgins W, Janowiak J, Mo KC, Ropelewski C, Wang J, Leetmaa A, Reynolds R, Jenne R, Joseph D (1996) The NCEP NCAR 40-year reanalysis project. B Am Meteorol Soc 77:437–472. https://doi.org/10.1175/1520-0477

Kanamitsu M, Ebisuzaki W, Woollen J, Yang SK, Hnilo JJ, Fiorino M, Potter GL (2002) NCEP–DOE amip-ii reanalysis (r-2). B Am Meteorol Soc 83(11):1631–1644. https://doi.org/10.1175/BAMS-83-11-1631

Katipoglu OM, Acar R, Senocak S (2021) Spatio-temporal analysis of meteorological and hydrological droughts in the Euphrates Basin, Turkey. Water Supp, ws2021019. https://doi.org/10.2166/ws.2021.019

Kite GW, Droogers P (2000) Comparing evapotranspiration estimates from satellites, hydrological models and field data. J Hydrol 229:3–18. https://doi.org/10.1016/S0022-1694(99)00193-6

Koch J, Demirel MC, Stisen S (2018) The SPAtial EFficiency metric (SPAEF): multiple-component evaluation of spatial patterns for optimization of hydrological models. Geosci Model Dev 11: 1873–1886. https://doi.org/10.5194/gmd-11-1873-2018.

Lang D, Zheng J, Shi J, Liao F, Ma X, Wang W, Chen X, Zhang M (2017) A comparative study of potential evapotranspiration estimation by eight methods with FAO Penman–Monteith Method in Southwestern China. Water 9:1–18. https://doi.org/10.3390/w9100734

Latrech B, Ghazouani H, Lasram A, M'hamdi BD, Mansour M, Boujelben A (2019) Assessment of different methods for simulating actual evapotranspiration in a semi-arid environment. Ital J Agrometeoro 2:21-34. https://doi.org/10.13128/ijam-650

Lauri H, Räsänen TA, Kummu M (2014) Using reanalysis and remotely sensed temperature and precipitation data for hydrological modeling in monsoon climate: Mekong River case study. J Hydrometeorol 15:1532–1545. https://doi.org/10.1175/JHM-D-13-084.1

Moorhead JE, Marek GW, Colaizzi PD, Gowda PH, Evett SR, Brauer DK, Marek TH, Porter DO (2017) Evaluation of sensible heat flux and evapotranspiration estimates using a surface layer scintillometer and a large weighing lysimeter. Sensors 17:2316–2350. https://doi.org/10.3390/s17102350

Moriasi DN, Arnold JG, Van Liew MV, Bingner RL, Harmel RD, Veith TL (2007) Model evaluation guidelines for systematic quantification of accuracy in watershed simulations. T ASABE 50(3):885–900. https://doi.org/10.13031/2013.23153

Paredes P, Martins DS, Pereira LS, Cadima J, Pires C (2017) Accuracy of daily PM-ETo estimations with ERA-Interim reanalysis products. Euro Water 59:239-246.

Piñeiro G, Perelman S, Guerschman JP, Paruelo JM (2008) How to evaluate models: observed vs. predicted or predicted vs. observed? Ecol Model 216(3-4):316–322. https://doi.org/10.1016/j.ecolmodel.2008.05.006

Purnadurga G, Kumar TL, Rao KK, Barbosa H, Mall RK (2019) Evaluation of evapotranspiration estimates from observed and reanalysis data sets over Indian region. Int J Clim 39(15):5791–5800. https://doi.org/10.1002/joc.6189.

Rienecker MM, Suarez MJ, Gelaro R, Todling R, Bacmeister J, Liu E, Bosilovich MG, Shubert SD, Takacs L, Kim GK, Bloom S, Chen J, Collins D, Conaty A, Silva AD, Gu W, Joiner J, Koster RD, Luccesi R, Molod A, Owens T, Pawson S, Pegion P, Redder CR, Reichle R, Robertson FR, Ruddick AG, Sienkiewicz M, Woollen J (2011) MERRA: NASA's modern-era retrospective analysis for research and applications. J Clim 24:3624–3648. https://doi.org/10.1175/JCLI-D-11-00015.1

Saha S, Moorthi S, Pan HL, Wu X, Wang J, Nadiga S, Tripp P, Kistler R, Woollen J, Behringer D, Liu H, Stokes D, Grumbine R, Gayno G, Wang J, Hou YT, Chuang HY, Juang HMH, Sela J, Iredell M, Treadon R, Kleist D, van Delst P, Keyser D, Derber J, Ek

M, Meng J, Wei H, Yang R, Lord S, van den Dool H, Kumar A, Wang W, Long C, Chelliah M, Xue Y, Huang B, Schemm JK, Ebisuzaki W, Lin R, Xie P, Chen M, Zhou S, Higgins W, Zou CZ, Liu Q, Chen Y, Han Y, Cucurull L, Reynolds RW, Rutledge G, Goldberg M (2010) The NCEP Climate Forecast System Reanalysis. B Am Meteorol Soc 91:1015–1058. https://doi.org/10.1175/2010BAMS3001.1

Salekin S, Burgess J, Morgenroth J, Mason E, Meason D (2018) A comparative study of three non-geostatistical methods for optimising digital elevation model interpolation. ISPRS Int Geo-Inf 7(8):300. https://doi.org/10.3390/ijgi7080300

Santhi C, Arnold JG, Williams JR, Dugas WA, Srinivasan R, Hauck ML (2001) Validation of the SWAT model on a large river basin with point and nonpoint sources. J American Water Resources Assoc 37(5): 1169-1188.

Santos JFS, Leite DC, Severo FAS, Naval LP (2020) Validating the Mark-HadGEM2-ES and Mark-MIROC5 climate models to simulate rainfall in the last agricultural frontier of the Brazilian North and North-East Savannah. Adv Res 21(8):43-54. https://doi.org/10.9734/air/2020/v21i830225

Sentelhas PC, Gillespie TJ, Santos EA (2010) Evaluation of FAO Penman-Monteith and alternative methods for estimating reference evapotranspiration with missing data in Southern Ontario, Canada. Agr Water Manage 97:635-644. https://doi.org/10.1016/j.agwat.2009.12.001

Seong C, Sridhar V, Billah MM (2018) Implications of potential evapotranspiration methods for streamflow estimations under changing climatic conditions. Int J Climatol 38 (2):896–914. https://doi.org/10.1002/joc.5218

Shi TT, Guan DX, Wu JB, Wang AZ, Jin CJ, Han SJ (2008) Comparison of methods for estimating evapotranspiration rate of dry forest canopy: Eddy covariance, Bowen ratio energy balance, and Penman-Monteith equation. J Geophys Res 113(D19):D19116. https://doi.org/10.1029/2008JD010174

Srivastava PK, Han D, Ramirez MAR, Islam T (2013) Comparative assessment of evapotranspiration derived from NCEP and ECMWF global datasets through Weather Research and Forecasting model. Atmos Sci Lett 14:118–125. https://doi.org/10.1002/asl2.427

Sun G, Noormets A, Chen J, McNulty SG (2008) Evapotranspiration estimates from eddy covariance towers and hydrologic modeling in managed forests in Northern Wisconsin, USA. Agr Forest Meteorol 148:257-267.

Tabari H, Grismer ME, Trajkovic S (2013) Comparative analysis of 31 reference evapotranspiration methods under humid conditions. Irrigation Sci 31:107–117. https://doi.org/10.1007/s00271-011-0295-z

TAGEM (2017) Türkiye'de sulanan bitkilerin bitki su tüketimleri. https://www.tarimorman.gov.tr/TAGEM/Belgeler/yayin/Tu%CC%88rkiyede%20Sulanan%20Bitkilerin%20Bitki%20Su%20Tu%CC%88ketimleri.pdf. Accessed: 16 March 2021

Tanguy M, Prudhomme C, Smith K, Hannaford J (2018) Historical gridded reconstruction of potential evapotranspiration for the UK. Earth Syst Sci Data 10(2): 951–968. https://doi.org/10.5194/essd-10-951-2018

Tian D, Martinez CJ, Graham WD (2014) Seasonal prediction of regional reference evapotranspiration based on Climate Forecast System Version 2. J Hydrometeorol 15:1166–1188. https://doi.org/10.1175/JHM-D-13-087.1

Tian Y, Zhang K, Xu YP, Gao X, Wang J (2018) Evaluation of potential evapotranspiration based on CMADS reanalysis dataset over China. Water 10:1126. https://doi.org/10.3390/w10091126

Tran TMA, Eitzinger J, Manschadi AM (2020) Response of maize yield under changing climate and production conditions in Vietnam. Ital J Agrometeorol, 1: 73-84. https://doi.org/10.13128/ijam-764

Türkeş 8M, (2020) Climate and Drought in Turkey. In: Harmancioglu, N., Altinbilek, D. (eds) Water Resources of Turkey. World Water Resources, vol 2. Springer, Cham. https://doi.org/10.1007/978-3-030-11729-0_4

Uppala SM, Kallberg PW, Simmons AJ, Andrae U, Bechtold VDC, Fiorino M, Gibson JK, Haseler J, Hernandez A, Kelly GA, Li X, Onogi K, Saarinen S, Sokka N, Allan RP, Andersson E, Arpe K, Balmaseda MA, Beljaars ACM, Berg LVD, Bidlot J, Bormann N, Caires S, Chevallier F, Dethof A, Dragosavac M, Fisher M, Fuentes M, Hagemann S, Hólm E, Hoskins BJ, Isaksen L, Janssen PAEM, Jenne R, Mcnally AP, Mahfouf JF, Morcrette JJ, Rayner NA, Saunders RW, Simon P, Sterl A, Trenberth KE, Untch A, Vasiljevic D, Viterbo P, Woollen J (2005) The ERA-40 re-analysis. Q J Roy Meteor Soc 131:2961–3012. https://doi.org/10.1256/qj.04.176

Willmott CJ (1981) On the validation of models. Phys Geogr 2(2):184–194. https://doi.org/10.1080/02723646.1981.10642213